A Gypsum-Barrier Design to Stop Seawater Intrusion in a Fractured Aquifer at Salento (Southern Italy)

M. J. Barcelona, M. Kim, and C. Masciopinto, R. La Mantia

Abstract **Seawater intrusion into fresh water aquifers occurs in many coastal hydrogeologic settings due to overexploitation of freshwater resources. It can be exacerbated by seawater level increases as a result of climate change on which there is wide consensus in the scientific community. Basin scale water balance deficits may be used together with hydrogeologic modelling and water quality monitoring data to track the advance of seawater intrusion.**

Due to the growth of population and increased exploitation of the ground water resources in coastal areas, the problem is truly global in proportion. The situation is particularly acute in the Mediterranean, the Yucatan peninsula in Mexico, the Middle East, the SE and SW United States as well as on many islands with arid to semi arid climates. Continued exploitation of limited freshwater resources can also lead to up flow of relict marine waters underlying the fresh water zone compounding the effects of seawater intrusion.

This study has been designed to test the feasibility of creating a subsurface barrier to seawater intrusion by induced gypsum precipitation in fractured carbonate aquifers. The barriers design was supported by laboratory experiments and by a mathematical model which simulated sweater intrusion in a costal aquifer at Salento, in Southern Italy. The results will assist regional, national, and local water management interests to better regulate water use and protection as well as to avoid conflicts over scarce resources.

Index Terms **Fractured aquifer, Seawater intrusion modelling, Gypsum barriers.**

Manuscript received September, 2006. This work was supported in part by the U.S. Department of … under Grant … and in part by AQUASTRESS EU Integrated Project (Contract no.: 511231-2).

M. J. Barcelona is with Department of Chemistry, Western Michigan University, 3442 Wood Hall, Kalamazoo, MI 49008, USA (e-mail: michael.barcelona@wmich.edu).

M. Kim was with Department of Chemistry, Western Michigan University. He is now with the Marine Environment Risk Assessment Research Division Korea, Ocean Research & Development Institute/SSI 391, Jangmok-ri, Jangmok-myon, Geoje 656-830, Korea (mkim@kordi.re.kr).

C. Masciopinto is with Consiglio Nazionale delle Ricerche, Istituto di Ricerca sulle Acque, Reparto di Bari, via Francesco De Blasio, 5, 70123 Bari, Italia (corresponding author: phone: +39-080-5820537; fax: +39-080-5313365; e-mail: costantino.masciopinto@ba.irsa.cnr.it)

R. La Mantia is with Consiglio Nazionale delle Ricerche, Istituto di Ricerca sulle Acque, Reparto di Bari, via Francesco De Blasio, 5, 70123 Bari, Italia (lamaros@libero.it).

I. Introduction

THE intrusion of seawater into coastal aquifers is a common problem in coastal zones of the world where increasing water requirements [1] and arid climate have induced overexploitation of groundwater [2]. Continued exploitation of limited freshwater resources can also lead to up-flow of relict marine waters underlying the freshwater zone compounding the effects of seawater intrusion [3].

Overexploitation of freshwater resources can render the ground water unfit for potable or agricultural use without extensive treatment. It can be exacerbated by seawater level increases as a result of climate change on which there is wide consensus in the scientific community [4]. Basin scale water-balance deficits may be used together with hydrogeologic modeling and water quality monitoring data to track the advance of seawater intrusion. Due to the growth of population and increased exploitation of the groundwater resources in coastal areas the problem is truly global in proportion [5]-[8].

Although many seawater intrusion studies have been carried out both around the world [9]-[12], and in the Salento Peninsula (Southern Italy) [13], very few of these studies have dealt with mathematical developments of seawater intrusion in fractured aquifers. On the Ionian coast of Southern Italy, a European experimental project [14] tested the efficacy of experimental grouting barriers, based on controlled sulphate crystallisation [15], in order to stop seawater intrusion into the coastal aquifer. One well-documented system aimed at minimizing seawater intrusion consists in the injection of reclaimed municipal wastewater [16], [17] into the coastal Salento aquifer [18]. However, it should always be remembered that a wide spectrum of technical and health challenges must be carefully evaluated prior to undertaking such a project [19]. For instance, Li et al. [20] observed that watertable accretion enhances beach erosion. However, artificial recharge, as recommended by the Water Framework Directive [21], is a useful supplementary measure in preventing and controlling groundwater pollution.

A simulation study of seawater intrusion at the Nardò aquifer in Southern Italy [18] has shown that the efficacy of the artificial recharge on the reversal of the seawater intrusion movement is not uniform along the coastline, due to variation of the groundwater discharge which outflows in the Ionian Sea. Indeed where the groundwater discharge is low the intrusion may reach 3000 m inland.

This work has simulated the modification of the extent of sweater intrusion due to possible interposition of gypsum barriers across the saturated zone along the coastal aquifer. Then the groundwater flow simulations allowed the definition of the seawater intruded zones when the artificial recharge at Nardò site is combined with sparingly soluble sulfate (gypsum) barriers. The model results were useful in order to design the optimal barrier positions and their lengths. Gypsum ($CaSO_4 \cdot 2H_2O$) was chosen to provide proof of concept for less soluble sulfates ($BaSO_4$) or phosphates which must be very carefully applied. The methodology for the preparation of gypsum over-saturated solution were based on the lab experiments carried out at CNR-IRSA (Bari, Italy) and at Western Michigan University (Kalamazoo, USA) laboratories; the determination of the location of the 50% salinity contour within the Nardò coastal aquifer (Southern Italy) and the zone of influence of an injection of the gypsum solution were obtained on the basis of a recently three-dimensional groundwater flow model of fractured coastal aquifer developed by CNR-IRSA.

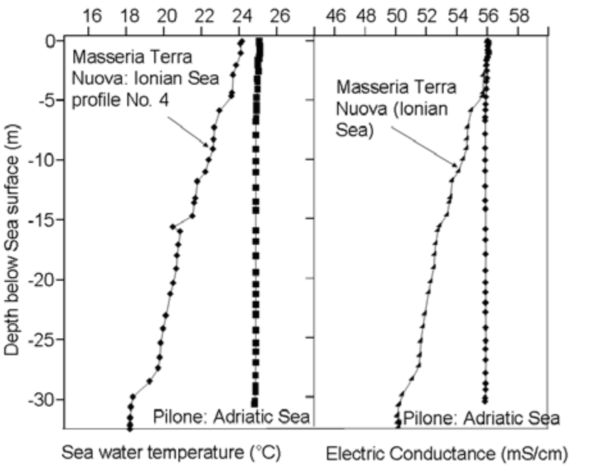

Fig. 2. Vertical profiles of the seawater during Summer 2004: the upward gradients of both Nardò temperature (on the left) and electric conductance (on the right) clearly showed the submarine spring outflows at location 4 and 5 of the Nardò site (see Figure 3).

II. Nardò aquifer

The Salento Peninsula consists mainly of sandstone, limestone and dolomite deposits. The Nardò aquifer is located at approximately 8 km from the Ionian Sea coastline. Geological studies [22] of the Nardò aquifer show that the limestone rock formations are significantly fractured and very permeable. As illustrated in Figure 1, Pleistocene deposits known as Calcareniti di Gallipoli (sandstone), with spatially variable thickness ranging from 5 to 7 m, are nearest to the ground surface. Below there is a formation with average thickness of 30 m, consisting of Calcare di Altamura (limestone) (Upper Cretaceous) intercalated by lenses of terra rossa (calcspar) and loamy sand. The underlying deposits are mainly limestone and dolomite. The water table is approximately 32 m below the ground surface, close to the sinkhole (see Figure 1). Fresh water floats over saline water intrusion from the Ionian Sea and it is confined within the

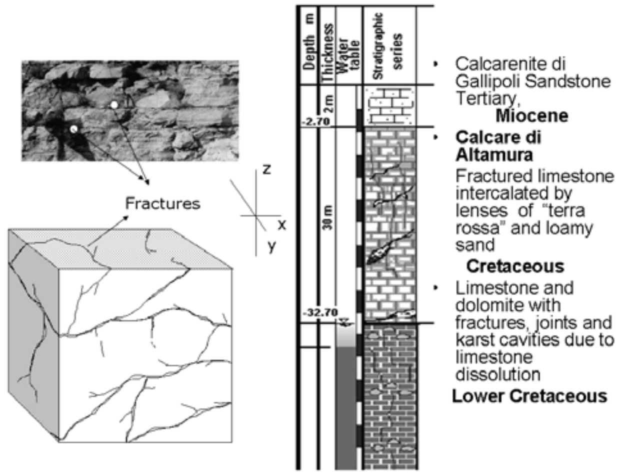

Fig. 1. Stratigraphic series at Nardò site in Southern Italy.

fractured limestone. Fractures are interconnected and partly filled with calcspar or terra rossa. Groundwater flows along preferential pathways within the aquifer under a piezometric head of approximately 3 m above the mean sea level. The preferential pathways are mainly horizontal conduits. The Pleistocene sediments are also fractured but the interconnected fractures are orientated along the local bedding planes.

The Nardò aquifer supplies fresh water to numerous households along the Ionian Sea coastline. Consequently, the water quality of the Nardò aquifer should be maintained at

TABLE I
QUALITY OF THE INJECTED WATER AND GROUNDWATER IN THE NARDÒ AQUIFER.

	Injected water[a]	Ground water[b] close the injection site			*Chidro* spring
	Mean	Min.	Mean	Max.	Mean
EC (μS/cm)	400	220	877	3000	6380
*p*H	7.75	6.5	7.3	7.9	7.23
Temperature (C)	17.8	14	15.4	17.7	24.0
$N\text{-}NH_4^+$ (mg/L)	Traces	0	0	Traces	0.0
$N\text{-}NO_2$ (mg/L)	0.03	0	0	0	0.0
$N\text{-}NO_3$ (mg/L)	8	0	6.8	18	14.6
Chloride (mg/L)	61	14	115	402	1585
DOC (mg/L)	47	0	12	41	5.02
TOX(μg/L as Cl)	25.5	0	7	28	nd[c]

[a]Average from 15 samples;
[b]Average from 64 samples collected from 7 sampling wells at Nardò site;
[c]nd: non-detected.

acceptable levels. The presence of organic compounds (revealed by dissolved organic carbon levels above 12 mg/L) together with an elevated concentration of chloride due to marine intrusion, makes the groundwater unfit for drinking purposes without treatment (See Table 1).

In previous work [3] a map of the salinity contour line shows the improvement of groundwater quality subsequent to injection into the sinkhole, which was started in 1991. In 2006 the groundwater salinity increased slightly with depth below the watertable with values in the range from 0.2 to 1.5 g/L. Also the salinity of Sea was monitored by means of electric conductance (EC), together with water temperature, *p*H and redox potential, collected in several locations along the coast (Table 2) by means of the Ocean Service (Idronaut) probe, which was able to draw these water constituent profiles up to 30 m below to the water table (Figure 2).

The sinkhole has been loaded in the past 15 years, by the Asso Channel which outflows municipal effluent from treatment plants and local surface drainages at a constant rate of about 140 L/s. In the coastal aquifer, the groundwater was sampled in monitoring wells located at different distances from the sinkhole, before and after 1991 when injection started (Table I).

The water samples were collected after ten minutes of pumping to ensure the removal of stagnant water in the pipelines. In wells without pumps, the water was collected by means of samplers located at 0.5-1 m below the watertable. The analytical methods utilized are reported in the Standard Methods [23]. Ten wells (3+7) were monitored from November 1953 to February 1954, 8 wells (6+2) during winter 1979/1980 and 14 wells (7+7) from November 1998 to March 1999. Water sampled from these wells confirmed a reduction of groundwater salinity owing to the injection of treated wastewater (see Table I). However, a general improvement in groundwater quality due to the reduction of ammonia and nitrites, was also observed coincident with increased nitrates, chemical oxygen demand (COD) and Total dissolved Organic Carbon (TOC) in the wells near the sinkhole.

Due to the presence of dissolved organic compounds and pathogens [24], the groundwater requires treatment to make it safe for drinking.

III. Numerical methods

In order to simulate the barriers effects on the Nardò groundwater flow, the fractured aquifer was idealized in a layered model [25], [26] made by several horizontal fractures bounded by impermeable sediments. This Nardò idealization was confirmed by tracer (Rhodamine-Wt and Iodine) tests carried out in the same aquifer, under pumping [27] and natural pressure gradient [28]. Each fracture is characterized by variable apertures which can be derived from the aquifer transmissivity values estimated in 49 wells of the study area, by mean stochastic methods [29]-[31].

In each fracture, we can define the interface position by considering the hydrostatic equilibrium of freshwater/saltwater pressures, based on the Ghyben-Herzberg equation.

TABLE II

Vertical profiles of the Ionian Sea water temperature (C), electric conductance, *p*H and redox potential (mV) (June 26, 2004) carried out by a boat with the multi-parameter probe (Ocean Seven) at 10 different geographic positions.

Sampling coordinates			Depth m	T (C)	EC mS/cm	*p*H	*E*h mV
Torre S. Isidoro							
1	N	40 13 16.7	0 3	24.377	55.215	7.72	-284
			1.4	23.945	55.762	7.77	-813
	E	17 55 30.1	2.0	24.059	56.093	7.82	-959
			2.4	24.055	56.127	7.82	-959
2	N	40 13 13.4	0 3	24.350	55.465	7.73	-705
			1 2	24.074	55.752	7.76	-802
	E	17 55 27.6	2.0	23.881	55.877	7.77	-894
			2 9	23.904	55.888	7.78	-961
3	N	40 13 08.0	0 1	24.460	55.832	7.75	-541
			0 2	24.486	55.900	7.75	-631
	E	17 55 13.2	0 9	24.566	56.517	7.77	-738
			1 1	24.543	56.528	7.77	-763
Masseria Torre Nuova							
4	N	40 09 52.2	0 3	24.085	56.180	7.78	-981
			5 9	22.969	54.954	7.79	<-1000
	E	17 56 10.5	20 3	20.521	52.309	7.81	<-1000
			31 5	18.239	50.144	7.81	<-1000
5	N	40 09 55.1	0 1	24.097	56.168	7.76	-422
			5 9	23.393	55.487	7.78	-574
	E	17 56 23.0	20 1	20.502	52.301	7.80	-817
			31.8	18.375	50.246	7.82	-981
6	N	40 10 02.4	0 1	24.267	56.399	7.76	-458
			5 9	23.544	55.627	7.76	-754
	E	17 56 37.8	10 3	22.488	54.503	7.79	-881
			16.7	20.661	52.468	7.82	<-1000
S. Maria al Bagno							
7	N	40 07 57.5	0 1	25.391	55.120	7.79	-416
			1.4	24.649	56.520	7.75	-610
	E	17 59 45.2	2.7	24.520	56.524	7.75	-657
			3 9	24.524	56.558	7.76	-699
8	N	40 07 55.2	0 1	24.619	56.706	7.70	-520
			1.4	24.585	56.528	7.76	-632
	E	17 59 40.4	2 1	24.573	56.509	7.75	-727
			3 5	24.373	56.399	7.75	-799
9	N	40 07 55.9	0 2	24.475	56.456	7.75	-396
			2.6	24.418	56.339	7.76	-542
	E	17 59 33.8	5.6	22.961	54.931	7.77	-640
			10.4	21.716	53.644	7.80	-882
Chidro spring							
10	N	40 18 17.3	0 3	23.964	55.684	7.70	-638
			1 1	23.801	55.551	7.80	-522
	E	17 40 57.3	1 2	23.798	55.748	7.80	-557
			2 3	23.824	56.025	7.79	-436

In addition, using the Dupuit assumption, we assume that inside the fractures freshwater flows in a horizontal direction [32]. In the proposed conceptual scheme all the fractures were assumed to have hydraulic connections between them and to have the same mean aperture b_m (*mm*), whereas the sharp interface approximates the 50% salt concentration contour line in the water.

The analytical solution of the interface position can be derived from integration of the Laplace (i.e., the continuity) equation in the generic vertical plane XZ, where the total freshwater outflow per unit of seacoast length Q_0 $(m^3/s/m)$ [30], can be derived from the solution of Navier-Stokes'

Equation for flow in a single fracture bounded by two parallel plates [33]:

$$Q(x) = -\frac{b_m^{\,2}}{12}\frac{\gamma_f}{\mu_f} n H(x) \frac{\partial \phi(x)}{\partial x} = \text{const} = Q_0 \quad (1)$$

where b_m is mean aperture of the horizontal fracture (mm); x = coordinate along the fracture length into the sea direction (m); γ_f/μ_f = specific weight/viscosity ratio of fresh water (= 10^7 $m^{-1}s^{-1}$ at 20 °C); $\phi(x)$ is the piezometric head of fresh water in x direction (m); $H(x)$ is the depth of the sharp interface below the sea (i.e., freshwater thickness) (m) and n = effective aquifer porosity (dimensionless).

Based on the analogy of Eq. (1) with Darcy's formula we can define the hydraulic conductivity of the aquifer as:

$$K = -\frac{b_m^{\,2}}{12}\frac{\gamma_f}{\mu_f} n \quad (2)$$

As known, n defines the uniform ratio of the void-space per unit volume of aquifer [34] and at section $x = 0$ it follows that:

$$n = \frac{\sum_{i=1}^{N_f} b_i}{B} \quad (3)$$

where Σb_i (m) is the sum of all the horizontal apertures in the vertical aquifer column with unitary horizontal area ($1x1$ m^2) and thickness B (m), while N_f is the total number of the fractures of the parallel set. In addition, as all fractures have been assumed to have the same mean aperture b_m (mm), it follows that, on average:

$$Q_0 = N_f Q_i = \frac{\sum_{i=1}^{N_f} b_i}{b_m} Q_i \quad (4)$$

where Q_i is the flow rate of the single fracture of the parallel set per unit of coast length.

Following the Ghyben-Herzberg formula, in every cross section at distance x, for $0 \le x \le L$, where L is the distance of coastline from the Ghyben-Herzberg interface toe position, the freshwater piezometric head H can be defined as:

$$H(x) = \phi \frac{\gamma_f}{\gamma_s - \gamma_f} = \delta\phi \quad (5)$$

and (1) can be written as:

$$Q_0 \times \partial x = -K \frac{H(x)}{\delta} \partial H(x) \quad (6)$$

Eq. (6) is a first order differential equation in x and H, which can easily be integrated between the section, $x=0$, at $H=B$, and the generic vertical cross-section x at $H=H(x)$:

$$Q_0 \times x = -K \frac{(B^2 - H(x)^2)}{2\delta} \quad (7)$$

At the outflow section, i.e., at $x=L$, we have $H(L)=H_s$ and:

$$Q_0 \times L = -K \frac{B^2 - H_s^2}{2\delta} = -n \frac{b_m^{\,2}}{12}\frac{\gamma_f}{\mu_f}\frac{(\delta\phi_0)^2 - H_s^2}{2\delta} \quad (8)$$

where H_s (m) is the depth (below the sea surface) of the sharp interface at the outflow section. Obviously, H_s=0 can also be set for zero discharge. The Ghyben-Herzberg interface is an approximate theory which considers that at outflow section is $H(L)$=0. This is of course not possible, and in the real situation we have an outflow *face* [32], where the water pressure almost abruptly decreases to zero, at the outflow section. Then, $H(L)$ = 0 doesn't mean that we do not have spring outflow but defines where the outflow takes place: i.e., 1) inland; 2) along the coastline or 3) offshore, below the sea surface.

Eq. (8) allows the sharp seawater/freshwater interface in the three-dimensional domain of the study area to be defined when the freshwater discharge at the coastline Q_0 is known. The reader should note that the origin ($x=0$) of L measurement is defined at the position where $\phi = \phi_0$ (or $H = B$).

Then the first step of computational operation consists of drawing the steady-date groundwater flow solution in each horizontal fracture of the parallel set. The latter was determined by solving the following partial differential equation [35], for steady-sate fluid flow through a two-dimensional fracture with spatially variable aperture:

$$\frac{\partial}{\partial x}\left[b^3(x,y)\frac{\partial \phi(x,y)}{\partial x}\right] + \frac{\partial}{\partial y}\left[b^3(x,y)\frac{\partial \phi(x,y)}{\partial y}\right] = 0 \quad (9)$$

subject to the following boundary conditions:

$$\phi(0,y) = \phi_0 \quad (9a)$$

$$\phi(L_x,y) = \phi_L \quad (9b)$$

$$\phi(x_j,L_y) = \phi_j \quad (9c)$$

$$\phi(x_j,0) = \phi_j \quad (9d)$$

$$\frac{\partial \phi}{\partial y}(x_i,L_y) = 0 \quad (6e)$$

$$\frac{\partial \phi}{\partial y}(x_i,0) = 0; \quad \text{with } i \neq j \quad (9f)$$

where x (L) is the coordinate along the fracture length; y (L) is the coordinate along the fracture width; ϕ (L) is the local piezometric head in the fracture; and b(x,y) (L) is the spatially-variable fracture aperture, which can be determined by means of pumping-well data [36]. Conditions 9a-9d impose the piezometric heads along the border nodes; conditions 9e-9f impose no-flux conditions in the border nodes where the piezometric heads are not assigned.

The finite difference method was used to discretize every horizontal domain of each fracture. The resulting set of equations has been solved by using the iterative successive-over-relaxation (SOR) method. Due to non-linearity of the Laplace (elliptic) equation, under non-laminar flow the system solution can be found only after linearization, at the second step. The error in the iterative method was less than 10^{-9} m. Simulation results for the seawater/freshwater interface are shown in Figure 3.

IV. Laboratory experimental tests

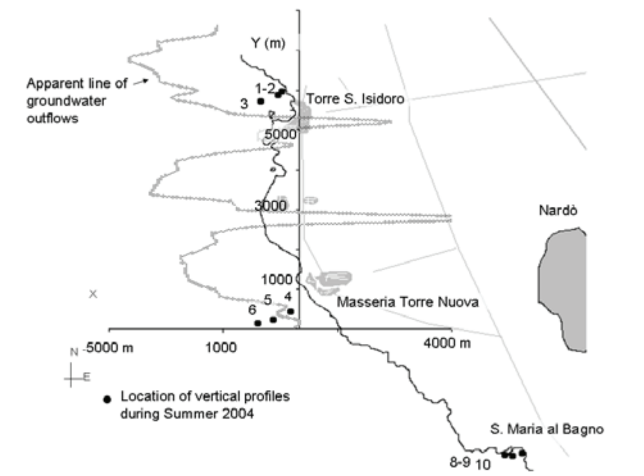

Fig. 3. Simulation result: Apparent stationary seawater-freshwater interface toe position in fractured aquifer subject to the artificial injection of 140 L/s and locations of the vertical Sea water temperature and electric conductance carried out during Summer 2004.

An interesting opportunity exists in the construction of physical barriers by using reactive gypsum ($CaSO_4 \cdot 2H_2O$) solutions resulting in precipitation in contact with high salinity solutions. If the precipitation process can be inhibited, then the spatial coverage of the physical barriers can be extended well beyond the injection wells. This approach has been successfully employed by Zeigenbalg and Crosby [37] and Zeigenbalg [38] to effect the immobilization of heavy metals and preventing inflow of brines into mining operations. To be effective in the Nardò aquifer we estimate that precipitation would have to be delayed for days to allow adequate penetration.

Preliminary gypsum precipitation experiments were conducted at CNR-IRSA (Bari) in >10-fold saturated $CaSO_4$ solutions (Figure 4). The course of the precipitation was followed by electrical conductance under active mixing and *p*H control. Polyacrylic acid (PAA) [39] and nitrilotrimethylene phosphonic acid (NTMP) [40] were evaluated as inhibitors at the micromolar level. Typical results (Figure 5) show the greater effectiveness of the NTMP over PAA in highly oversaturated gypsum solutions. Realistically, however, the practical direction must be to conduct injections of gypsum solutions those of or other sparingly soluble salts into brackish water where contact with the diluted seawater will drive the degree of supersaturation up.

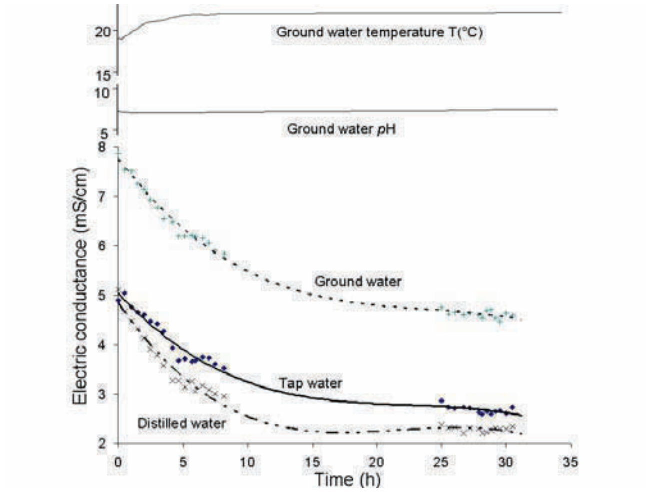

Fig. 4. Laboratory tests of hemihydrate ($CaSO_4 \cdot \frac{1}{2}H_2O$) gypsum precipitation in groundwater, tap water and distilled water at initial constant temperature (16 C) and *p*H (7.2).

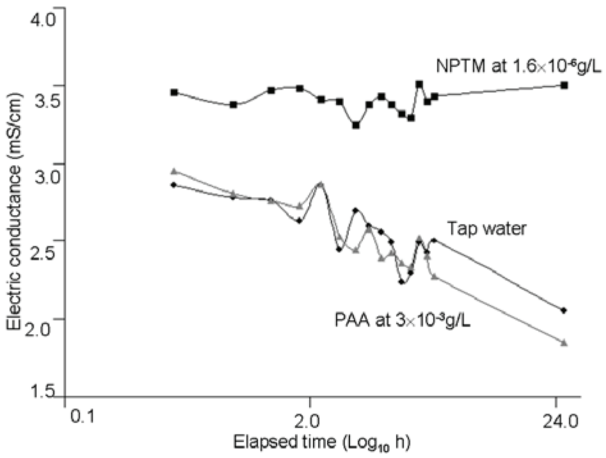

Fig. 5. Batch test results showing the efficacy of some compounds (PAA and NTMP) on gypsum precipitation in an oversaturated hemihydrate tap water solution.

In the late seventies, Barcelona et al. [41] and Barcelona and Atwood [42], [43] conducted studies on the effects of natural organic matter on the precipitation of gypsum in hypersaline seawater evaporation ponds and coastal seawater.

They demonstrated that natural organic matter at levels below 5 mg-C/L could inhibit gypsum precipitation in over-saturated seawater solutions. Lipid materials, long-chain hydrocarbons and fatty acids, were shown to sorb and effectively block growth of the 111 (Ca) monoclinic crystal plane which inhibited nucleation and precipitation and resulted in the formation of larger tabular crystals rather than rhombic needles. These results and that of more recent scaling inhibition work by Dogan et al. [39] further suggest that it could be possible to control the injection of over-saturated $CaSO_4$ solutions with lower levels of organic inhibitors than those used by Zeigenbalg and Crosby [37].

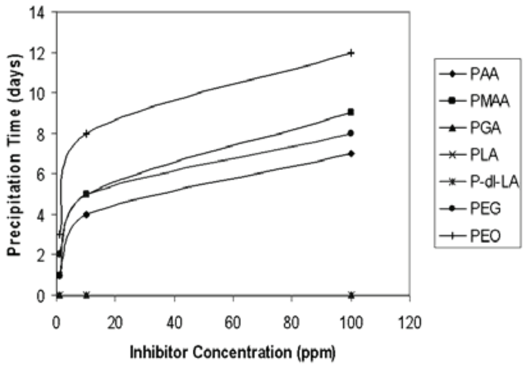

Fig. 6. Effects of inhibitors on gypsum precipitation time in 90% seawater/10% freshwater solutions.

More recent experiments have been made in 90% (V/V) synthetic seawater to which 10% (V/V) 5M $CaCl_2$ solutions was added. The course of these experiments was followed by a differential electrical conductance measurement technique with matched conductance electrodes. Each electrode was suspended in a thermal jacketed pyrex tall-form beaker, one with the synthetic seawater alone and one with the mixed seawater and calcium chloride solution. The output of the electrodes was input to a data logging Analog-Digital signal processor (OMEGA ADI28) interfaced with a PC which, after scaling, created an Excel file of the sample minus reference values. This approach was made necessary by the high conductance of seawater which made direct conductance measurement relatively insensitive to the signal change caused by precipitation of gypsum.

A series of non-toxic, polymeric compounds including: PEO (polyethylene oxide), PEG (polyethylene glycol), PMAA (polymethyl acrylic acid), PLA (polylactic acid), P-d,l-LA (poly-d,l-lactic acid), and PGA (polyglycolic acid), was tested. The results of these early experiments are shown in Figure 6. Clearly, the PEO, PMAA, PEG, and PAA were the most effective inhibitors of gypsum precipitation in the part-per-million concentration range. Of the four polymers, PEG and PEO would be the most cost-effective (based on reagent grade chemical costs of $100 to 180/kg). However, technical food-grade chemical costs would be much lower as would potential natural substitutes such as gelatin or partially hydrogenized keratin which have seen some testing as inhibitors. Of note here is that NTMP has been found to be an effective inhibitor of the far less soluble $BaSO_4$

V. Simulation results

Simulation results allowed the definition of the region of groundwater affected by seawater intrusion even considering the artificial recharge of 140 L/s (Figures 7-8). It should be noted that the vertical profiles of seawater temperature measured in the Ionian Sea at positions no. 4 and 5 on Figure 3, agreed with the apparent position of the submarine groundwater outflow (see Figure 2 and Table II) estimated by simulation results. The model flow solutions have been used to define the gypsum barriers position and their length (about 500 m) along the sea coast, i.e. the barriers were located in the region of low hydraulic conductivity, as reported in Figure 7a. Figure 7b exhibits the modification of the 50% seawater/freshwater zones due to the presence of the gypsum barriers.

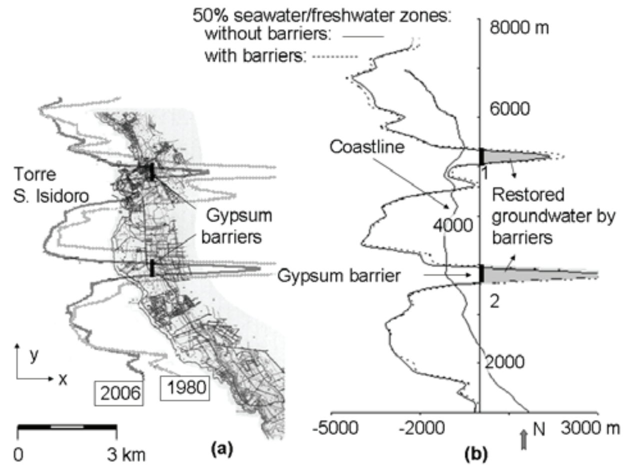

Fig. 7. Simulation results: Comparison of the seawater intrusion lines at Torre S. Isidoro: (a) during 1980 (i.e. without artificial recharge) and during 2006 (actual, by injecting 140 L/s) and (b) by inserting 2 artificial gypsum barriers of 500 m of length across the saturated thickness (40 m).

Each barrier was included in the numerical code by assuming that the gypsum precipitation will produce high hydraulic resistance to the groundwater flow with a reduction of 10% of aquifer outflow discharge Q_0 at coast line from 0.83 L/s to 0.74 L/s at barrier 1 (y=5000 m) and from 0.53 L/s to 0.48 L/s at barrier 2 (y=3000 m). This effect produced an increase of piezometric head which achieved 0.2 m in the grid nodes of the barriers (Figure 8). Based on simulation results the position X_d (m) of contour line of the piezometric head $\phi = \phi_0 = 1$ m with respect to the coastline was defined. This value was used into equation (8) together with other experimental estimations, i.e. ratio δ (=30), average transmissivity (0.0475 m^2/s) of the parallel set of the fractures and their number N_f (=40) in order to determine the extents of seawater intrusion L (m) at every position defined by grid ordinate y. These latter were estimated also during 1980, i.e. before the recharge operation started on 1991 (Figure 7a).

The flow simulation results including the barriers (see Figure 8b) showed an increase of apparent extent of the intrusion, at both the barrier positions y=3000 m and y=5000 m, due to the reduction of groundwater discharge at coastline. In the actual situation, instead, the seawater is stopped at the barrier positions, which are supposed to have elevated flow resistances artificially created by gypsum precipitation. The total groundwater volume of the Nardò aquifer, which can be restored by gypsum barriers was estimated approximately at 250,000 m^3, i.e. 500×(2000+3000)/2×40×0.005, where 0.005 is the Nardò aquifer storativity [3]. Furthermore the barriers did not produced significant modifications of extent of seawater intrusion in the others coastal zones of the region. The total groundwater outflowed into the Ionian Sea during 2006 was estimated to be 193 L/s without the barrier and 183 L/s with the barriers. This means that the difference of 10 L/s may increase the volume annually stored into the Nardò aquifer of about 0.3 million m3/y, by improving the efficiency of artificial recharge.

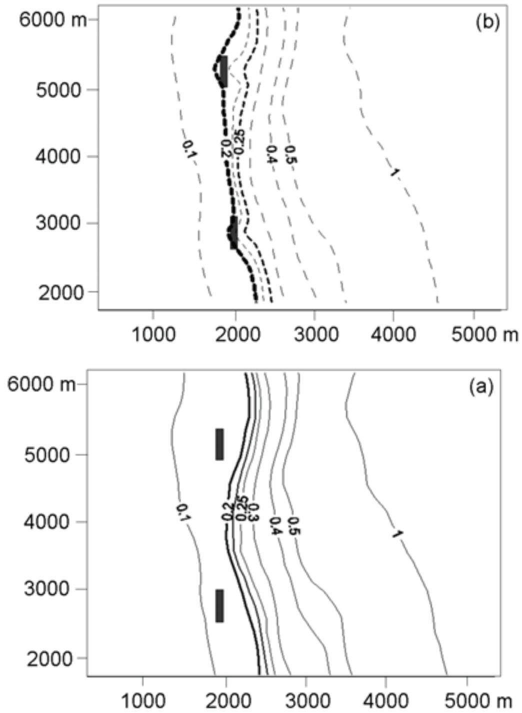

Fig. 8. Simulation results: (a) piezometric contour lines (in meter above average sea level) during 2006 and their modifications (b) due to 2 apparent gypsum barriers of 500 m of length across the saturated aquifer thickness (40m).

The simulations of the groundwater flow carried out for the Nardò coastal aquifer defined the stationary seawater-freshwater interface in a fractured aquifer subject to the artificial injection of 140 L/s and estimated by how much the extent of seawater intrusion could be reduced by inserting a vertical impermeable barrier across the saturated aquifer thickness. The apparent position of the line of the submarine groundwater outflow was also verified by means vertical profiles of seawater temperature and electric conductance, which were carried out during Summer 2004 in 10 locations of the Ionian Sea. Furthermore experimental lab tests have shown the feasibility of the barriers by injecting in wells assigned oversaturated solutions of gypsum hemihydrate ($CaSO_4 \cdot ½H_2O$), together with additional compound able to delay the induction time of gypsum crystal formation into the fractures. The length of 500 m and the positions of the barriers were identified by model simulation results, as they were positioned in the groundwater zones where the groundwater flow was very low. The simulation code defined also the possible modification of the groundwater flow by inserting the apparent impermeable barriers and estimated a possible increase of 0.3 million m^3/y of the stored volume artificially injected into groundwater. The estimated retained groundwater volume which may be saved by gypsum barriers was estimated to be about 0.25 million m^3/y. These volumes could be very useful for irrigation purposes, although treatment of pumped water from wells is required, before drinking. The improvement achieved in the Nardò area should encourage the local Authority to implement new recharge-barrier projects into these coastal and arid regions.

NOMENCLATURE

b_i spatially-dependent local fracture aperture [L];

b_m mean aperture of the parallel set of horizontal fractures [L];

B maximum saturated aquifer thickness [L];

$\sum b_i$ sum of the all horizontal apertures in the vertical aquifer column with unitary horizontal area (1×1 m^2) and thickness B [L];

g gravity acceleration (Lt^{-2});

H(x) depth of the sharp interface below the sea (i.e., freshwater thickness) [L];

H_s depth (below the sea surface) of the sharp interface at the outflow section [L];

i,j extremity nodes of the generic channel of computational grid (-);

K hydraulic conductivity of the set of parallel fractures [Lt^{-1}];

L distance of coastline from the Ghyben-Herzberg interface toe position [L];

L_{id} estimated position where the freshwater outflow takes place (i.e., L_{id}=L if the intrusion extent is equal to 0) [L];

L_i extent of the seawater intrusion (=L-L_{id}) with respect to the coastline [L];

N_f total number of the fractures of the parallel set (-);

n aquifer effective porosity (-);

Q_i flow rate of single fracture of the parallel set per unit of coast length [L^2t^{-1}];

Q_0 fresh water discharged into the sea per unit of coast length [L^2t^{-1}];

Q_{ij} grid channel flow rate [L^2t^{-1}];

T hydraulic transmissivity of the parallel set of fractures [L^2t^{-1}];

X_d position of the seawater intrusion with respect to y axis [L].

Greek letters

δ freshwater/seawater-freshwater specific weights ratio(-);
$\Delta\phi$ piezometric head difference [L];
Δx, Δy step size of computational grid [L];
ϕ, ϕ_0, ϕ_i, ϕ_j groundwater piezometric head [L];
γ_f specific weight of freshwater [$ML^{-2}t^{-2}$];
γ_s specific weight of seawater [$ML^{-2}t^{-2}$];
μ_f dynamic viscosity of freshwater [$ML^{-1}t^{-1}$]..

ACKNOWLEDGMENT

Thanks are due to the Regional Customs Safeguard Police (Guardia di Finanza), Ministry of the Interior, for technical support given at the IRSA during the vertical profiles realization into Ionian and Adriatic Sea. Also, we appreciate the experimental assistance of Brendan Sanchez, who was an ACS (American Chemical Society) PROJECT SEED (Science Experience for Economically Disadvantaged Students) in the WMU Chemistry Department.

REFERENCES

[1] Masciopinto, C., Barbiero, G. and Benedini, M. 1999. A large scale study for drinking water requirements in the Po basin (Italy), Water International, 24 (3), 211-220.

[2] Park C.-H. and Aral M. M. 2004. A multi-objective optimisation of pumping rates and well placement in coastal aquifers. Journal of Hydrology, 290, 80-99.

[3] Masciopinto C. 2006. Simulation of coastal groundwater remediation: the case of Nardò fractured aquifer in Southern Italy. Environmental Modelling & Software, 21, 85-97.

[4] Oreskes, N. 2004. The Scientific Consensus on Climate Change. Science, 306, December 2004.

[5] SWICA2, Salt Water Intrusion and Coastal Aquifers. 2003. Proceedings of the Second International Conference on Salt Water Intrusion and Coastal Aquifers: Monitoring, Modeling, and Management 3/30-4/2/03 Merida, Yucatan, Mexico Sponsored by the Mexican Academy of Science and the Autonomous University of Mexico.

[6] Barlow P.M. and Wild E.C. 2002. Bibliography on the Occurrence and Intrusion of Salt Water in Aquifers along the Atlantic Coast of the United States, U.S. Geological Survey Open file Report 02-235, 35pp.

[7] Framing Committee of the GWSP 2004. The Global Water System Project: Science Framework and Implementation Activities, Earth System Science Partnership Project, Global Water System Project, Bonn, Germany.

[8] European Environment Agency 1996. Seawater Intrusion in Coastal Aquifers, section 3.7 in Problems in Europe, Topic Report, No. 15.

[9] Oude Essink, G.H.P. and Boekelman, R.H. 2000. Saltwater intrusion in coastal aquifers. In Groundwater Pollution Control. Ed. by K. L. Katsifarakis, WIT Press, Boston, 145-201.

[10] Oude Essink, G. H. P. 2001. Improving freshwater supply problems and solutions. Ocean & Coastal Management, 44, 429-449.

[11] Bear J. and Bensabat J. 2003. Analysis of grouting performance. Proc. IV meeting on crystallization technology for prevention of salt water intrusion, September 26-29, 2002 - Scanzano Joinico (Matera, Italy). GEO-GRAPH publishing Company, Segrate (Milano, Italy), 32-38.

[12] Bower, J. W., Motz, L. H., Duden, D. W. 1999. Analytical solution for determining the critical conditions of saltwater upconing in a leaky artesian aquifer. Journal of Hydrology, 221, 43-54.

[13] Cotecchia, V., Tadolini, T. and Tulipano, L. 1974. The results of research carried out on diffusion zone between fresh water and seawater intruding the land mass of Salentine Peninsula (Southern Italy). Proc. Inter. Symp. on Hydrogeology of volcanic rocks, Isole Canarie, Lanzarote (Spain), 1-15.

[14] Polemio, M. and Gallicchio, G. 2003. Proc. IV meeting on crystallization technology for prevention of salt water intrusion, September 26-29, 2002 - Scanzano Joinico (Matera, Italy). GEO-GRAPH S.n.c. publishing Company, Segrate (Milano, Italy), 75.

[15] Gomis-Yagües, V., Boluda-Botella, N. and Ruvia-Beviá, F. 1999. Gypsum precipitation dissolution as an explanation of sulphate concentration during seawater intrusion. Journal of Hydrology, 228, 48-55.

[16] Asano T. 2002. Multiple uses of water: reclamation and reuse. GAIA, 11 (4): http://www.gaia-online.net/.

[17] Masciopinto, C., Palmisano, N., Tangorra, F. and Vurro, M. 1991. A decision support system for artificial recharge plant. Water Science and Technology, 24 (9), 331 342.

[18] Masciopinto C. and Carrieri C. 2002. Assessment of water quality after 10 years of reclaimed water injection: the Nardò fractured aquifer (Southern Italy). Ground Water Monitoring & Remediation, 22 (1), 88-97.

[19] Asano T. and Cotruvo J. 2004. Groundwater recharge with reclaimed minicipal wastewater: health and regulatory considerations. Water Research, 38, 1941-1951.

[20] Li L., Barry D.A., Pattiaratchi C.B. and Masselink G. 2002. BeachWin: modelling groundwater effects on swash sediment transport and beach profile changes. Environmental Modelling & Software, 17, 313-320.

[21] European Community Directive (ECD) 2000. Water Framework Directive 2000/60. European Parliament and of the Council of 23 October 2000. Establishing a frameworks for Community action in the field of water policy. Official Journal of the European Communities, 22-12-2000.

[22] Grassi, D., Tadolini, T. and Tulipano, L. 1975. Influenza delle caratteristiche morfologico - strutturali e paleogeografiche sull'idrologia della zona situata a nord di Otranto (penisola salentina). Atti del 3 Convegno Internazionale Sulle Acque Sotterranee, Palermo, 1-5 settembre, 1975.

[23] Standard Methods for the Examination of Water and Wastewater - 19th. 1995. American Public Health Association, 1015 fifteenth Street, NW Washington, DC, 20005, 9-99, 9-102.

[24] Masciopinto C., La Mantia R., Carducci A., Casini B , Calvario, A., Jatta, E. 2006. Unsafe tap water in households supplied from groundwater in the Salento Region of Southern Italy. Journal of Water and Health, 5 (1), 129-148.

[25] Essaid, H. I. 1990. A multilayered sharp interface model of coupled freshwater and saltwater flow in coastal systems: model development and application. Water Resources Research, 26 (7), 1431-1454.

[26] Kazemi, H. and Gilman, J. R. 1993. Multiphase flow in fractured petroleum reservoirs. In Bear, J., Tsang Chin-Fu and De Marsily, G. Flow and contaminant transport in fractured rock, Academic Press, Inc. London, 6-19, 270-272.

[27] Troisi S., Vurro M. and Di Fazio A. 1985. Studio metodologico di parametri idrodisperivi mediante misure in situ. Quaderni IRSA, 69, Rome (Italy).

[28] Masciopinto, C., Benedini, M., Troisi, S., and Straface, S. 2000. Conceptual models and field test results in porous and fractured media. In Groundwater Pollution Control. Ed. by K. L. Katsifarakis, WIT Press, Boston, 245-270.

[29] Moreno, L., Y.W. Tsang, C.F. Tsang, V. Hale and Neretnieks, I. 1988. Flow and tracer transport in a single fracture: a stochastic model and its relation to some field observations. Water Resources Research, 24, 2033-2048.

[30] Dagan, G. 1989. Flow and transport in porous formations. Springer-Verlag, Berlin (Germany), 465.

[31] Brown, S. R. 1987. Fluid flow through rock joints: The effect of surface roughness. Journal of Geophysical Research, 92 (B2), 1337-1347.

[32] Bear J. and Verruijt A. 1987. Modeling Groundwater Flow and Pollution, D. Reidel Publishing, Dordrecht, Holland, 196-206.

[33] Bear J. 1972. Dynamics of fluids in porous media. American Elsevier publishing Company, INC. New York, 126,164-165.

[34] Borgia G.C., Bortolotti V., Masciopinto C. 2002. Valutazione del contributo della porosità effettiva alla trasmissività di acquiferi fratturati con tecniche di laboratorio e di campo. IGEA-Groundwater Geoengineering, 17, 31-44.

[35] Chrysikopoulos C.V. and James S.C. 2002. Transport of neutrally buoyant and dense variably sized colloids in a two-dimensional fracture with anisotropic aperture. Transport in Porous Media, 51, 191-210.

[36] Masciopinto C. 2005. Pumping-well data for conditioning the realization of the fracture aperture field in groundwater flow models. Journal of Hydrology, 309 (1-4), 210-228.

[37] Zeigenbalg G. and Crosby K.S. 1997. An Overview of a Pilot Test to reduce brine inflows with controlled crystalization of gypsum at the IMC Kalium K2 Brine Flow. Mineral Resources Engin, 6 (4), 173-184.

[38] Zeigenbalg G. 1999. In-situ remediation of heavy metal contaminated soil or rock formations and sealing of water inflows by directed and controlled crystallization of naturally occurring minerals. In R.F. Rubio (Ed.) Mine Water and Environment. Int'l Congress Seville, SP p. 667-672.

[39] Doğan Ö., Akyol E. and Öner M. 2004. Polyelettrolytes inhibition effect on crystallisation of gypsum. Cryst. Res. Technol., 39 (12),1108 1114.

[40] Klepetsanis P.G. and Koutsoukos, P.G. 1998. Kinetics of calcium sulphate formation in aqueous media: effect of organophosphorus compounds. Journal of Crystal Growth, 193, 156-163.

[41] Barcelona M.J., Tosteson T.R. and Atwood D.K. 1976. Study of organic-calcium interactions: gypsum precipitation in tropical surface water. Marine Chemistry, 4, 89-92.

[42] Barcelona M.J. and Atwood D.K. 1978. Gypsum-organic interactions in natural seawater: effect of organics on precipitation kinetics and crystal morphology. Marine Chemistry, 6, 99-115.

[43] Barcelona M.J. and Atwood D.K. 1979. Gypsum-organic interactions in the marine environment: sorption of fatty acids and hydrocarbons. Geochimica et Cosmochimica Acta, 43, 47-53.